AN EXPERIMENTAL AND NUMERICAL STUDY OF THE CRACK PROPAGATION BEHAVIOUR IN AISI 304L AUSTENITIC STAINLESS STEEL UNDER THERMAL FATIGUE.

P. Bouin[1,2,3], C. Gourdin[1,2], A. Fissolo[1,3], S. Marie[1]
[1]CEA, DEN, DM2S, SEMT, LISN, F-91191 Gif-sur-Yvette, France.
[2]LaMSID, UMR EDF-CNRS-CEA 2832.
[3]GPM ERMECA, UMR CNRS 6634, INSA Rouen, France.
E-mail of corresponding author: pauline.bouin@cea.fr

ABSTRACT

The incident of the Civaux I power plant as some works in thermal fatigue have disproved current methodologies and usual criteria to predict propagation when components are submitted to thermal fatigue. Improvements in analytical methodologies and new experimental data are required to get better assessments of crack propagation under thermal fatigue.

As part of this work, a new thermal fatigue test, Fat3D, has been developed to study the problem of fatigue crack growth under thermal fatigue conditions on AISI 304L quasi-structure specimens. The importance of the initiation and the propagation phases on a notched specimen and the evolution of the stress intensity factor according to the propagation were also investigated. This experimental campaign has also been completed by a characterisation campaign on the AISI 304L material and by a benchmark of different non destructive techniques to detect and follow crack propagation.

In parallel, numerical analyses have been developed using the French finite element code of the CEA, Cast3M. This combined experimental and numerical study enables to evaluate the proposed improvements in analytical methods to accurately predict crack growth under thermal loadings and to understand the influence of the main parameters concerning crack propagation in such components.

INTRODUCTION

In their in-service life, several components such as train wheels, engine pistons, moulds, brazing of electrical devices or turbine blades are submitted to cyclic loadings which have thermal origins [1]. In nuclear power plants, thermal fatigue has firstly been observed in Fast Breeder Reactor (FBR) and then, in some components of Pressurised Water Reactors (PWR) [1, 2].

In the case of the water leakage which occurred in 1998 in Civaux Unit 1, the thermal fatigue damage was due to an incomplete mixing between cold and warm fluids along a mixing tee [3]. Some analyses demonstrated the risks of thermal fatigue phenomena and raised the problem of the extension of uniaxial mechanical fatigue results to predict thermal fatigue resistance of the components [4]. Previous works on thermal fatigue have shown that a crack network with or without a dominant crack could be reproduced under pure cyclic thermal loadings for representative conditions in laboratory [5]. The present study focuses on the crack propagation under pure cyclic thermal loadings. The new design of Fat3D experiment has been developed to understand the mechanism of crack propagation.

The first part of this paper presents the principles and the experimental methodology of the thermal fatigue test, Fat3D. The second part introduces the first results of FAT3D. Finally, the last part of this paper deals with the finite element analysis of the experiment and the discussion of the results.

PRINCIPLES OF THE THERMAL FATIGUE TEST

The aim of the Fat3D experiment is to make a crack propagate under a thermal 3D loading on a quasi-structure specimen. This quasi-structure specimen, a pipe, is placed inside a six heating-rod furnace. It is supported

by a mounting fixture which does not involve additional stress on it. Fig. 1 (a) shows a scheme of the thermal test bench.

After a first heating ramp up to a reference temperature, some water at room temperature is injected on the internal surface of the pipe and creates a parabolic cooling zone. The external surface stays heated during the entire test. The repeated thermal shocks result in two types of temperature gradients:

- Local temperature gradients due to temperature differences between the inner and outer surfaces of the specimen.
- Global temperature gradients resulting from temperature differences between the different sides of the specimen.

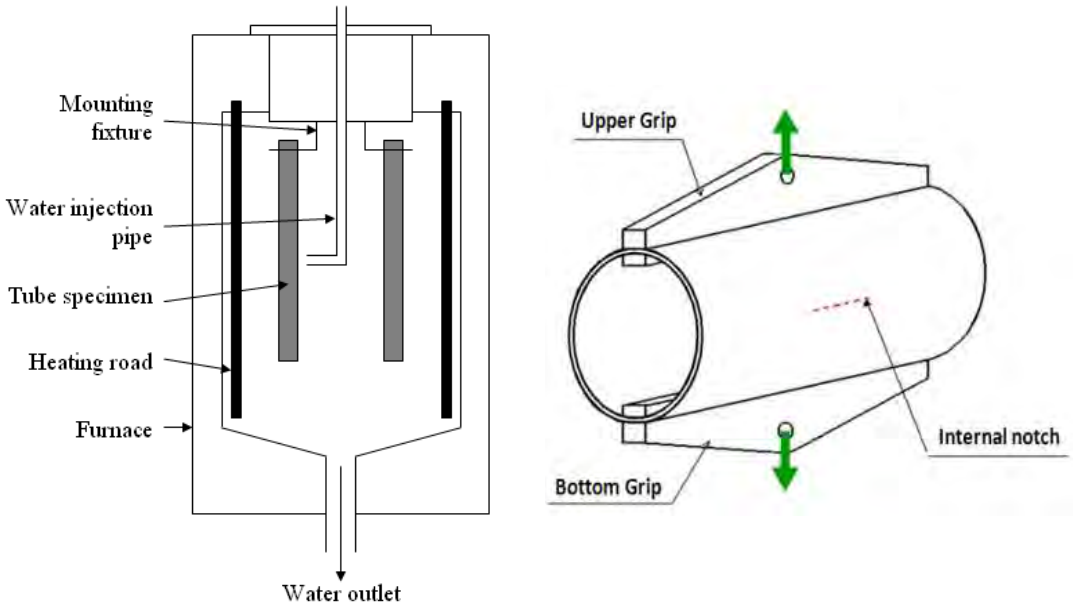

(a) (b)

Figure 1: Schematic of the Fat3D test bench (a) for thermal cycling (b) for mechanical marks.

The thermal cycling is regularly stopped in order to characterise the crack evolution using Non Destructive Control (NDC) techniques as liquid penetrant testing and optical analysis using an endoscope. The crack growth is assessed from the crack length differences measured on the internal surface between two thermal cycling stops.

Between thermal cyclings, mechanical marks are also realised and the crack propagation is assessed using post-mortem pictures of the crack. To carry out these mechanical marks, a mechanical fatigue loading is imposed on the tube. The loading ratio is kept constant and positive. Figure 1 (b) presents the mechanical test bench.

Concerning the loading cycle itself (Fig. 2), it may be divided into two phases included a cooling part and a heating part. The cooling phase mainly depends on the water injection time tf and the water injection temperature Tf. As regard to the heating phase, it is mostly influenced by the total cycle time tc and the furnace setting temperature Tc. Thus, the main loading parameters kept to control the Fat3D experimental tests are:

- tc, the total cycle time.
- tf, the water injection time, corresponding to the cooling duration.
- Tc, the furnace temperature. It should be noticed that this latter corresponds to the temperature set point of the rod furnace and not to the maximum specimen temperature.

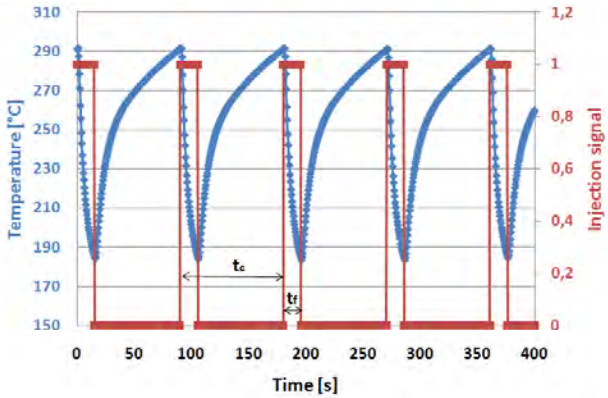

Figure 2: Evolution of the temperature of the quasi-inner thermocouple in front of the injection and injection signal according to the time (tc=90s, tf=15s).

The other primary parameters influencing the test results correspond to the tube dimensions, i.e. the specimen height h and thickness t, and the initial crack size a0 and c0. As the aim of the test is to study propagation, thick geometries are retained.

SPECIMEN DESIGN AND INSTRUMENTATION

All the specimens are taken from a 304L stainless steel pipe. Table 1 presents the chemical composition of the material. This pipe complies with all the RCC-MR specifications [6]. The tube specimens are 320mm long, 167mm in outer diameter and 17mm thick. The inner and outer surfaces are machined to obtain a final roughness Ra of 3.2, which is representative of PWR surface finishes.

Table 1: Chemical composition of 304L.

Alloy	C	Cr	Ni	Mo	Mn	Si	N	S	P
% mass	< 0,03	18 à 20	10 à 12	0	< 2	< 1	< 0,11	< 0,015	< 0,045

Thermal characterisation specimen

Concerning this first type of specimen, six groups of four thermocouples are placed on an external generating line. The investigated thicknesses are 16mm, 10mm, 5mm in depth, while the last set of thermocouples is positioned on the outer surface (Fig. 3 (a)). The chosen heights are 20, 90, 130, 150, 165 and 240 mm from the bottom of the tube. Two other external thermocouples are added at two heights: 55 and 290 mm from the bottom. To fix the thermocouples to the tube, holes have been drilled and ceramic glue is used. The signals are analysed at a 10 Hz frequency using a PCI-6036E card with a SCXI1000 box.

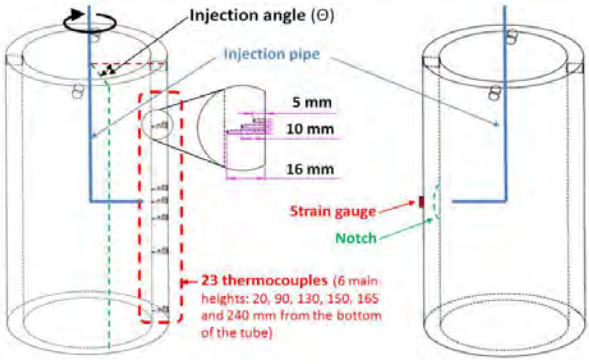

(a) (b)

Figure 3: (a) Geometry of thermal profile characterisation specimen. Four thermocouples (three in the thickness and one at the surface) are located at different heights; (b) Geometry of the test specimen.

Test specimen

To focus the test on the crack propagation, a second type of specimen is used. It consists in a pipe tube with a longitudinal semi-circular notch which is milled in the internal surface of the specimens (Fig. 3 (b)). The notch centre is placed in front of the injection pipe (hj=160mm), half way up. On top of some thermocouples, a high temperature strain gauge Kyowa KHCS-10-120-G12-16C2MW is added on the outer surface, at the opposite of the notch.

THERMAL FATIGUE TEST RESULTS

Thermal characterisation results

Three basic loadings have been investigated for the thermal characterisation: tc=120s, tf=20s; tc=90s, tf=15s and tc=60s, tf=10s. Figure 4 (a) represents the local thermal gradients for a total cycle time of 90s. This last thermal loading was a good compromise between total cycle time and thermal gradient. The maximum temperature evolution for a total cycle of 90s is shown on Figure 4 (b). The cooling of the internal surface leads to a decrease of the temperature inside and close to the cooling zone.

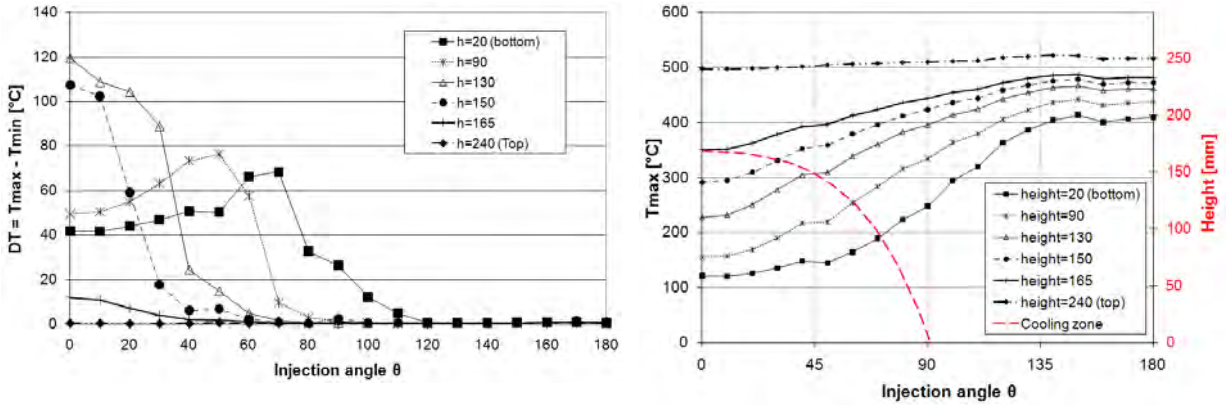

(a) (b)

Figure 4: Evolution of the temperature gradients for each internal thermocouple (a) and evolution of the maximum of temperature for each internal thermocouple (b) as a function of the injection angle (tc=90s, tf=15s).

Propagation test results

A first test was carried out alternating thermal loadings to make the crack propagate with mechanical loadings to mark the front. The initial crack dimensions were a0=5mm and c0=42mm. The thermal loading parameters were Tc=650°, tc=90s and tf=15s. Concerning the mechanical cycling, the maximum load was 210kN which corresponds to an estimation by finite element analyses of a maximum stress intensity factor of ~15MPa.m^0.5 at the crack tip. The number of cycles, i.e. 5000 cycles, is chosen to obtain a maximum front crack increment of 100µm.

Finally, six fatigue cycles have been conducted:
- 10000 thermal fatigue cycles,
- 5000 mechanical fatigue cycles (R=Fmin/Fmax=0.1),
- 5000 thermal fatigue cycles,
- 5000 thermal fatigue cycles,
- 5000 mechanical fatigue cycles (R=Fmin/Fmax=0.4),
- 15000 thermal fatigue cycles.

Figures 5 and 6 show the evolution of the crack on the internal surface at different steps of the propagation test. The crack lengths are only the minimum values as it is assumed that the closed parts are possibly not observable during the surface inspection. Moreover, no cracks are detected at the bottom of the notch. Thermal stripping (crack network on the surface) seems to have appeared between 20000 and 35000 cycles (Figure 5 (b) and (c)).

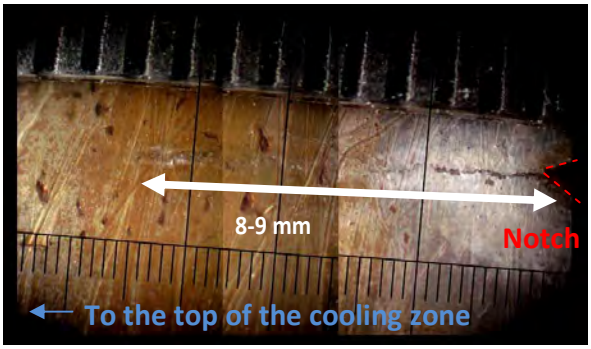

(a)Top crack (after 10000 thermal cycles)

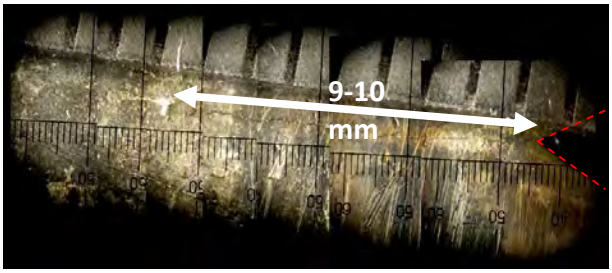

(b)Top crack (after 20000 thermal cycles)

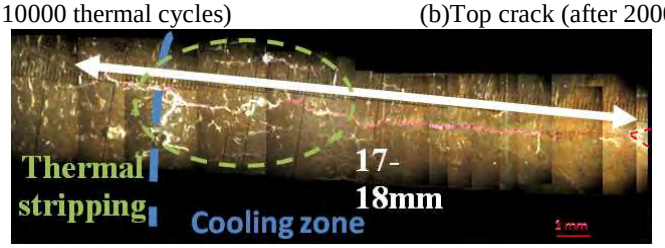

(c)Top crack (after 35000 thermal cycles)

Figure 5: Evolution of the crack on the top of the notch.

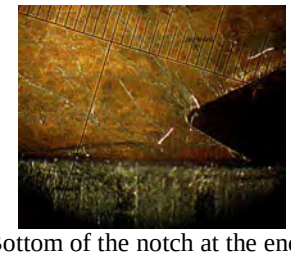

Figure 6: Bottom of the notch at the end of the test.

Figure 7 represents two post-mortem views of the specimen tube. It confirmed (see below) that the visual inspection of the internal surface underestimate the real crack front, in particular, in the direction of the bottom of the tube. In Figure 7, the presence of the mechanical marks is underlined by the green and blue lines. The red line represents the initial notch.

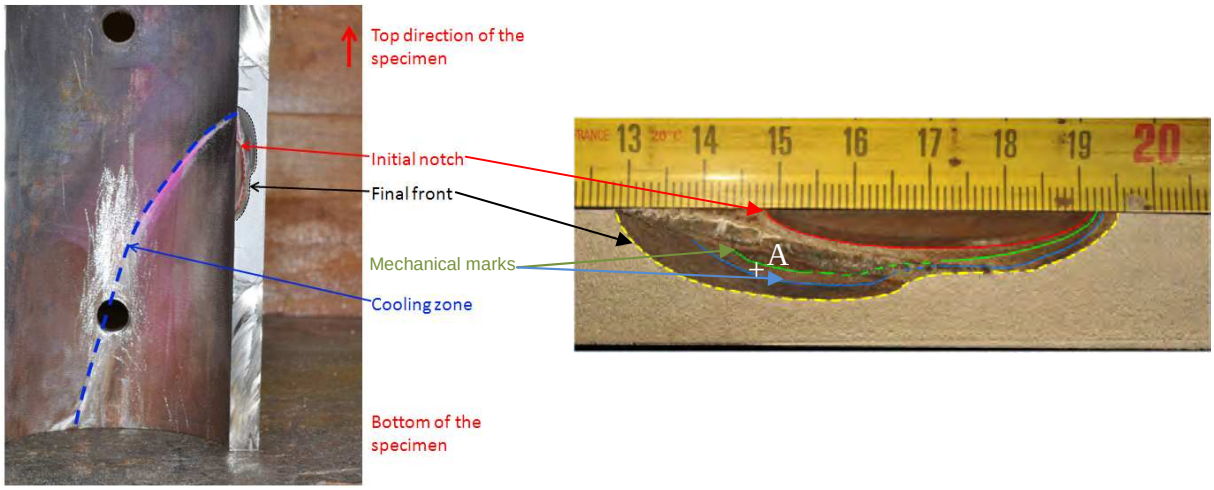

(a) General post-mortem view (b) Detail of the crack front

Figure 7: Post-mortem view of the specimen after 35000 thermal cycles.

Scanning Electron Microscopy (SEM) study

Figure 8 presents the typical fracture structure of the post-mortem crack observed using a SEM (this particular picture was taken at point A on Figure 7). Striations of about 0.1µm can be seen. Using the work of Kimura [7], a value of 3.10-7 m/cycle for crack growth is estimated which corresponds to a SIF range of 30-40 MPa.m^0.5 (Figure 9). It is remembered that the temperature around the notch, at the top of the cooling zone is about 300°C (Figure 4).

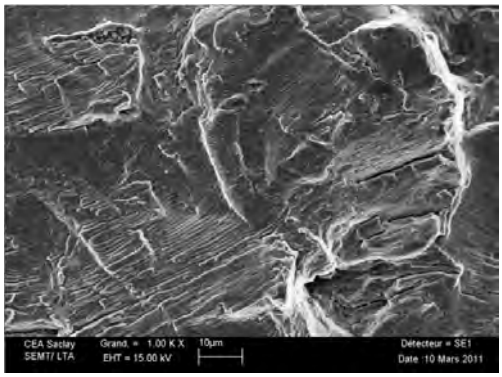

Figure 8: Typical SEM picture of the post-mortem crack.

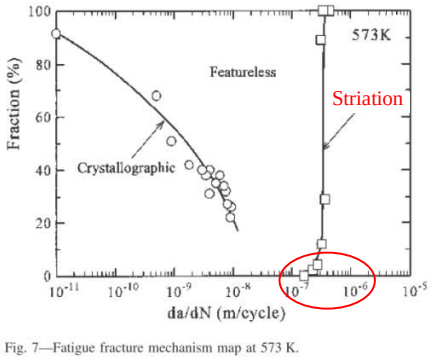

Fig. 7—Fatigue fracture mechanism map at 573 K.

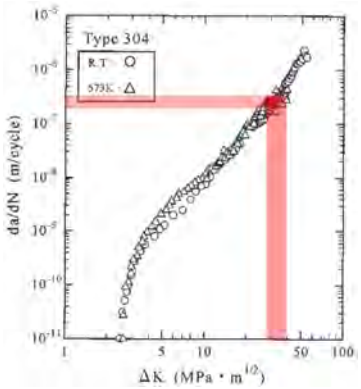

(a) Fatigue fracture mechanism map at 300°C. (b) da/dN vs ΔK for the type 304 steel.

Figure 9: Evaluation of the SIF range for 304 steel at 300°C [7].

NUMERICAL ANALYSIS

Thermal cycle model

Concerning the modelling of the propagation, it assumed that the thermal and mechanical calculations can be uncoupled. To determine the thermal loading, a first mesh is realised taking into account the specific geometry of the cooling zone.

Three types of thermal transfer are considered:

- The radiation between the furnace heating rod and the external tube surface and between the different inner tube surfaces are characterised by the emissivity of the tube (ε) and the radiation temperatures (Tray);
- The convection between the hot air and the tube is defined by the air convection coefficient (Hair) and the furnace temperature (Tc). Concerning the thermal shocks, the convection is dependent on the water convection coefficient (Heau) and the injection water temperature (Tf);
- Conduction inside the tube is determined by the coefficient of conduction (K);

Mechanical model

In the following calculations, the material is considered as isotropic and elastic. To realise the mechanical analyses, the stabilised thermal results are projected on the mechanical mesh which contains the semi-elliptical crack (Fig. 10). To take the symmetries into account, nodal displacements perpendicular to the symmetric plane are blocked. Crack propagation is modelled using a strategy of remeshing of the crack front.

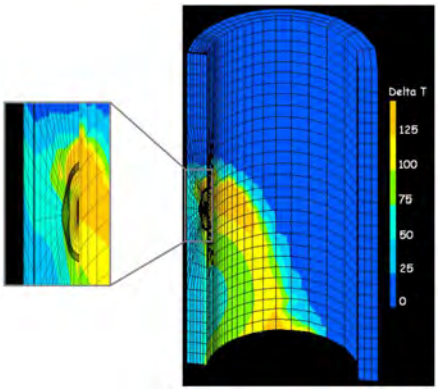

Figure 10: Mesh of the crack propagation specimen and distribution of the thermal local gradient.

Crack growth prediction

To assess the crack growth [8], the energy release rate J is first calculated using the Cast3M operator G_Theta [9]. The stress intensity factor range is then calculated along the front crack according to the following equation:

$$\Delta K_J^{\,2} = \Delta J^2 * E \qquad \text{(Eq. 2)}$$

$$\text{With } \Delta J = J\max - J\min \qquad \text{(Eq. 3)}$$

Then, the crack growth per cycle is assessed by using the Paris law (Eq. 4) at each node of the crack front [10]. The initial crack length is considered sufficient to apply it. The crack propagation law can be defined as follows:

$$\frac{da}{dN} = C(\Delta K_J)^n \qquad \text{(Eq. 4)}$$

Finally, the crack growth prediction is realised by propagating the crack from the initial front using finite element analyses. The initial crack geometry is a semi-ellipse which crack length is c0=42mm and a0=5mm. Then, the stress intensity factor range ΔK is calculated along the front. Its maximal value is identified to determine the number of cycles dN_i required to make the crack propagate of a da_i. To determine the new front geometry, the crack growth is calculated at each front node. It is assumed that the crack growth of each node is normal to the front. The front is updated and a new propagation step is launched.

Figure 11 presents first simulations results according to the time. The unsymmetrical propagation is due to local temperature gradients which decrease more quickly on one side than the other (Figure 10). The numerical results seem to present the same tendency on the evolution of the crack front as the experimental propagation (Figure 11). Some works, especially on taking into account plasticity correction at the crack front, are currently investigated. This could lead to a better agreement between experimental and numerical results.

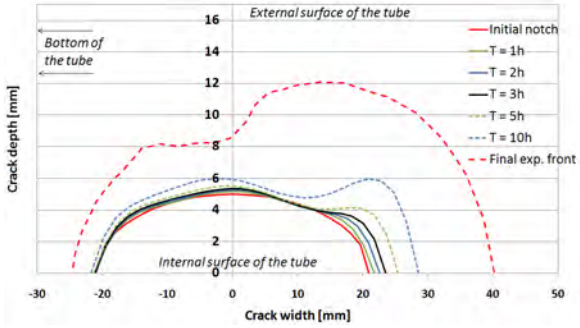

Figure 11: Crack growth prediction (tc = 90s, tf = 15s).

FURTHER WORKS

A campaign of thermal tests has been launched with different loadings and initial notches. A second test, with the same geometry and the same loadings is currently carried out to see the repeatability of the results.

Concerning the assessment of the crack dimensions as part of the NDE technique benchmark, an ultra-sonic study is made on the characterisation specimen. To improve the finite element analysis, plasticity correction will be integrated into the post treatment of the data.

CONCLUSION

The new Fat3D experiment shows its possibilities in crack propagation under pure thermal loadings. It is possible to obtain significant thermal gradients to make a crack propagate. It is also possible to have indications and assessment of this propagation, and in particular, by using mechanical beach marks.

The finite element analysis developed using the Cast3M code is qualitatively in agreement with the first experimental results. However, the simulation could be improved by taking the plasticity correction into account.

Finally, both experimental and numerical works on 304L tubes will enable to improve existing methods to accurately assess the crack growth propagation under pure thermal loads in austenitic stainless steel pipe.

ACKNOWLEDGMENTS

This work is published by permission of the French Atomic Energy Commission.

REFERENCES

[1] Fissolo A., Fissuration en fatigue thermique des aciers inoxydables austénitiques, CEA Report R-5982, Mémoire d'Habilitation à Diriger les Recherches; 2001. Université des Sciences et Technologie de Lille.
[2] Nulife project, Pilot project on thermal fatigue – item 3, Document D(08) 25383, December 2008.
[3] Cipière M.F., Le Duff J.A., Thermal fatigue experience in French piping. International Insitute Of Welding, Document n°XIII-1981-01, Lubjana, 2001.
[4] Fissolo A., Amiable S., Ancelet O., Mermaz F., Stelmaszyk J.M., Constantinescu A., Robertson C., Vincent L., Maillot V., Bouchet F., Crack initiation under thermal fatigue: An overview of CEA experience. Part I: Thermal fatigue appears to be more damaging than uniaxial isothermal fatigue, International Journal of Fatigue, Volume 31, Issue 3, March 2009, pp. 587-600.
[5] Ancelet O., Chapuliot S., Hennaf G., Marie S. Development of a test for the analysis of the harmfulness of a 3D thermal fatigue loadings in tubes. Internal Journal of Fatigue; 2007;29: pp. 549–64.
[6] AFCEN, French code RCC-MR: Règles de conception et de construction des matériels mécaniques des îlots nucléaires RNR, 2002.
[7] Kimura M., Yamaguchi K., Kobayashi K., Matsuoka S., Takeuchi E., Fatigue fracture mechanism maps for a type 304 stainless steel. Mettallurgical and materials transactions A; 2004; 35A: pp. 1311-1316.
[8] Chapuliot S., Nédélec M. Analytical method for the calculation of J parameter on cracked pipes under thermal loading and mechanical plus thermal loading, ASME PVP 2002, Vancouvert, Canada.
[9] Cast3M documentation. http://www-cast3m.cea.fr/; 2008.
[10] Paris P.C., Gomez M.P., Anderson W.E., A rational analytic theory of fatigue. The trends in Engineering, 13, No. 1, pp. 9-14.